Orbital Parameters of 80 Nearby Mildly Metal-Poor Stars : a search for correlations between abundance ratios and kinematics

E. Jehin, F. Bancken

Institut d'Astrophysique et de Géophysique, Université de Liège, Belgium

Abstract: Orbital characteristics of 80 HIPPARCOS mildly metal-poor stars are derived assuming a sligthly modified Ostriker and Caldwell (1979) Galactic model. A comparison with other studies is performed and relations between the dynamical properties of the stars and their well-known spectroscopic abundances are investigated. We pay a special attention to the 21 stars of Jehin et al. (1999).

1 Introduction

The chemical composition of unevolved metal-poor stars provides important information about the nucleosynthesis processes during the early galactic evolution. As these low mass stars do not dissipate orbital energy the knowledge of their kinematics provides new "fossil" information with which to explore various formation scenarios (Johnston et al. 1996).

2 The Galactic Mass Model

We have adopted a slightly modified Ostriker and Caldwell (1979) model, whose components are:

- a **central mass**,
- a **flattened disk** whose surfaces of equal density are oblate spheroids,
- a spherical **bulge-halo**,
- a spherical **dark halo**.

The Ostriker and Caldwell's surface disk has been replaced by a flattened disk in order to simplify the numerical orbit computations. We chose a density law that reproduces, by projection on the Galactic plane, Ostriker and Caldwell's surface density. We assume the Galaxy to be axisymmetric.

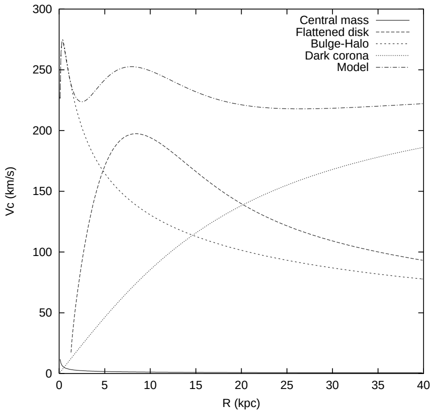

Figure 1: Contributions of each component to the Rotation Curve.

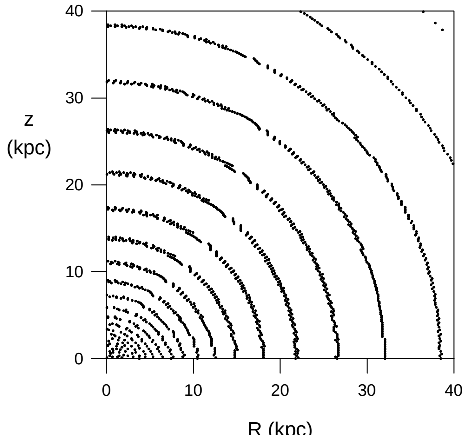

Figure 2: Isopotential contours in the meridional plane.

2.1 The Density Laws

- **Flattened Disk**

  We adopt the following density profile ρ_d for the disk component

$$\rho_d(m) = \rho_{d,0} \frac{e^{-m}}{\sqrt{m}} \tag{1}$$

  where $m = \sqrt{(\frac{R}{a})^2 + (\frac{z}{c})^2}$.

  R and z are the usual cylindrical coordinates, a and c being respectively the scale length and height of the disk.

- **Spherical bulge-halo**

  The bulge-halo density profile, ρ_{bh}, is given by

$$\rho_{bh}(r) = \begin{cases} \frac{\Sigma_0}{\pi n} \left\{ \frac{u+3}{\sqrt{u}} \mathrm{arctg}\left(\sqrt{u}\right) - 3 \right\} \frac{1}{u^2} & \text{if } r > n \\ \frac{4\Sigma_0}{15\pi n} & \text{if } r = n \\ \frac{\Sigma_0}{\pi\, n} \left\{ \frac{3-u}{\sqrt{u}} \ln\left(\frac{1+\sqrt{u}}{\sqrt{1-u}} \right) - 3 \right\} \frac{1}{u^2} & \text{if } r < n. \end{cases}, \tag{2}$$

  where $u = |(\frac{r}{n})^2 - 1|$, n is the core radius and Σ_0 the central surface density of the bulge-halo.

- **Spherical Dark Halo**

  Finally, the density profile of the dark halo is

$$\rho_{dh}(r) = \frac{\rho_{dh,0}}{1 + (\frac{r}{r_{dh}})^2} \tag{3}$$

  where $\rho_{dh,0}$ is the central value and r_{dh} the core radius of the dark halo.

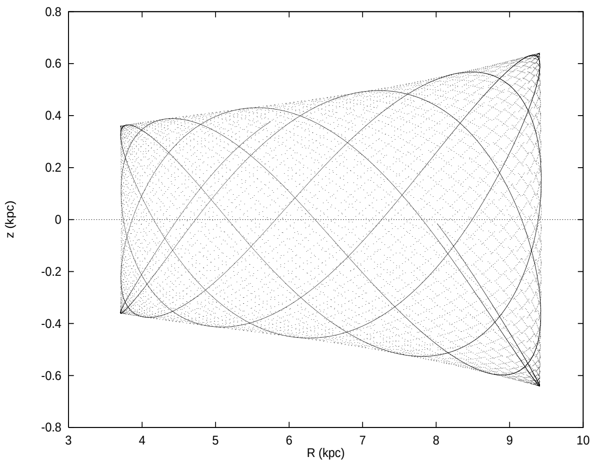

Figure 3: HD22879 meridional orbit.

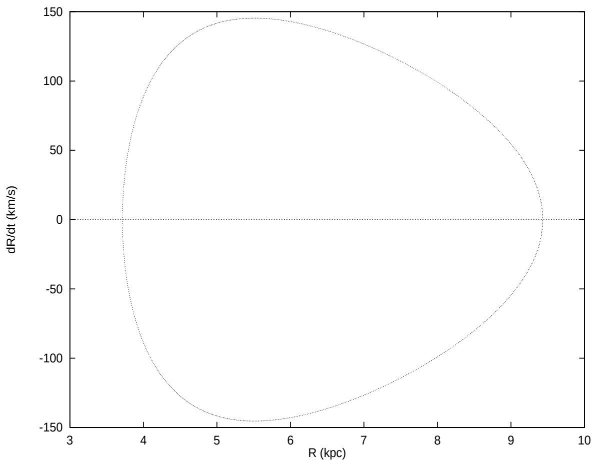

Figure 4: HD22879 horizontal surface of section.

2.2 ROTATION CURVE

We used the Ostriker and Caldwell's values for the parameters in the density laws (1)-(3), and we adjusted the contribution of each component in order to obtain the best possible agreement with the observed rotation curve as is usually done. We used the Allen and Santillàn (1991) observational data for the rotation curve. The contributions to the rotation curve of each component are shown in Fig. 1.

2.3 THE POTENTIAL

The potential of each component is calculated numerically from the Poisson's equation $\Delta\Phi = 4\pi G\rho$. The resulting isopotential contours in the meridional plane are shown in Fig. 2.

3 The Data

The data sample was built from 3 different studies giving high quality abundance ratios of nearby unevolved metal-poors stars. These stars have a metallicity around [Fe/H] ~ -1, which corresponds approximately to the transition between the halo and the disk.
The 21 stars taken from Jehin et al. (1999) have high precision abundance ratios of 16 elements. Nissen and Schuster (1997) derived accurate abundances for 11 elements and have computed orbits with the model of Allen and Santillàn (1991) for 25 disk and halo stars. The 40 most metal-poor ([Fe/H] < -0.6) F and G disk stars come from the large study of Edvadsson et al. (1993), where they have obtained accurate abundances of a douzen elements in a differential analysis with respect to the sun, and the orbital parameters using a three-component Myamoto potential.

The new parallaxes and proper motions are available in the HIPPARCOS Catalogue (ESA, 1997). The σ_π/π is better than 15% for all these stars (except for 5 stars from Nissen and Schuster, 1997) with a mean error of 5.5% for all the sample. Proper motions errors only reach 2%. The radial velocities were selected from several sources: Barbier-Brossat et al. (1994), Evans (1967) and Wilson (1953). They are known to about 2 km/s for most of the stars.
We applied a systematic correction to the abundance ratios, based on stars which are common

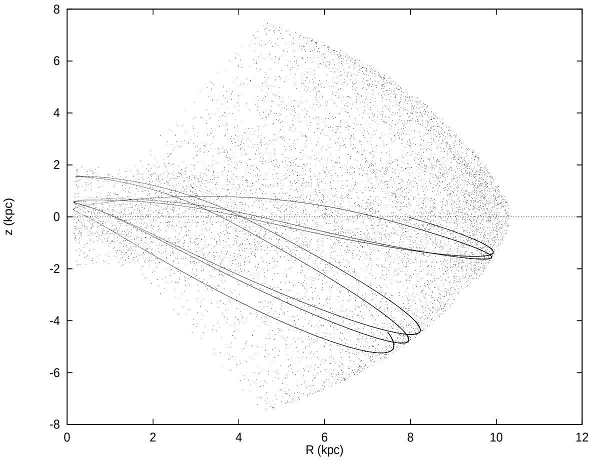

Figure 5: HD193901 meridional orbit.

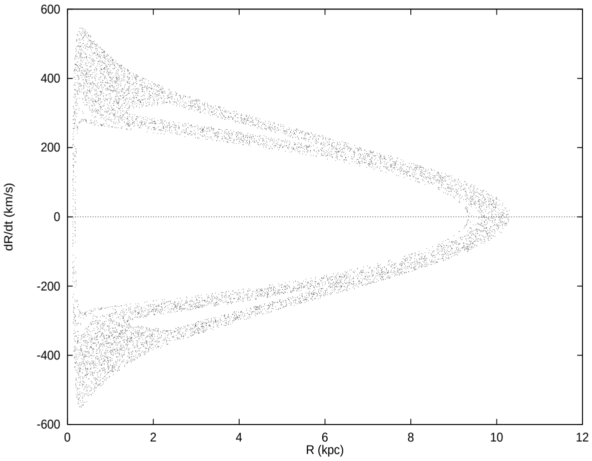

Figure 6: HD193901 horizontal surface of section.

with the analysis of Nissen and Schuster (1997).

4 Galactic space velocities

We calculate the Galactic space velocities U (radially outwards), V (in the direction of the Galactic rotation), W (vertically upwards) and their errors with respect to the local standard of rest using the method presented in Johnson and Soderblom (1987). The corrections applied to the observed velocities taking into account the solar motion are (-10.4, +14.8, +7.3) km/s in (U,V,W) (Mihalas and Routly, 1968). The solar galactocentric distance and circular velocity were taken to be 8.0 kpc and 220 km/s, respectively.

For each star our calculations were carried out during 1000 crossings of the Galactic plane. We used time steps of 10^4 years and at the end of most orbital trajectory the total energy was conserved to $\mid \Delta E/E \mid < 10^{-4}$. We maintained the z-component of the angular momentum at its initial value throughout the computation. We determined the area covered by the orbit in the meridional plane (R,z) as well as horizontal and vertical Poincarés surface of section. Both regular (box, tube, etc.) and chaotic orbits were found as it is illustrated in Fig. 3 to 6.

During the integration of the orbit only a fraction of the positions of the star are recorded, so it defines a background area in the meridional plane. In order to get an idea about the actual trajectory we overplotted the beginning of the orbit's path whose duration is approximately 500 million years, as shown in Figs. 3 and 5 for two stars.
In the horizontal surface of section, a (R, dR/dt) point has been plotted each time the star crossed the Galactic plane upwards. The results for two stars are shown in Figs. 4 and 6.

Orbital characteristics such as R_{min} (the minimum projected distance to the Galactic center), R_{max} (the maximum projected distance to the Galactic center), eccentricity taken as $(R_{max} - R_{min})/(R_{max} + R_{min})$, and Z_{max} (the maximum heigth reached by the star over the Galactic plane) were computed, as well as the errors on these parameters. Monte Carlo simulations show that the mean relative errors for the stars with box-orbit type are around 1% for R_{min} and R_{max}, 7% for the eccentricity and 7.7% for Z_{max}. The results for the 21 stars from Jehin et al. (1999) are listed in table 1.

Star	U	V	W	Rmin	Rmax	Exc	$\lvert Z_{max} \rvert$
	km/s	km/s	km/s	kpc	kpc		kpc
22879	98.36	−70.97	−37.11	3.69	9.39	0.436	0.636
25704	118.63	−49.50	1.44	4.21	10.38	0.423	0.057
59984	19.33	−36.24	−10.81	5.53	8.07	0.187	0.146
61902	−80.07	17.71	−31.50	6.71	11.59	0.267	0.634
63077	135.33	−43.40	46.89	4.29	11.49	0.457	1.048
63598	−39.46	−71.50	9.89	3.91	8.20	0.354	0.137
76932	38.23	−76.80	77.39	3.99	8.22	0.347	1.614
78747	−20.41	16.88	−18.56	7.79	9.33	0.090	0.282
79601	9.35	−18.72	−29.12	6.58	8.03	0.099	0.412
97320	−83.37	−5.22	−30.28	6.08	10.46	0.265	0.543
111971	7.83	17.55	30.87	7.99	9.28	0.075	0.488
126793	2.99	15.15	−7.15	8.03	8.92	0.052	0.103
134169	−26.66	12.72	22.12	7.65	9.27	0.096	0.346
152924	−34.98	−11.53	20.66	6.67	8.62	0.128	0.300
189558	−84.12	−113.76	50.62	2.41	8.89	0.574	1.023
193901	145.69	−230.16	−66.03	0.12	10.42	0.978	7.531
194598	66.11	−262.10	−23.53	0.68	8.44	0.851	0.501
196892	−12.17	−113.75	−26.24	2.48	8.06	0.530	0.395
199289	37.84	−51.77	−11.21	4.76	8.30	0.271	0.159
203608	2.69	58.83	13.47	8.00	13.49	0.255	0.296
215257	55.35	29.86	52.98	7.38	11.86	0.233	1.166

Table 1: Galactic velocity components with respect to the LSR and the computed orbital parameters for the sample of Jehin et al. (1999).

5 Correlation with abundances

I our attempt to find some correlation between kinematics and abundance ratios, we confirm in Fig. 7, with our new data and computations, the relation found by Nissen and Schuster (1997) between the abundance ratio [Ni/Fe] and Z_{max} (or R_{max}), the maximum height above the Galactic plane reached by the star in its orbit. We find similar correlations for [Na/Fe] and the [α-elements/Fe] ratios. The results could be explained by assuming that these stars have been accreted from low density regions of the outer halo, where the chemical evolution proceeds more slowly than in the inner halo (Nissen and Schuster 1997). However, the stars with peculiar [Na, Ni, α/Fe] ratios are also characterized by very small perigalactica ($R_{min} < 1.5$ kpc), as shown in Fig. 8, and high eccentricity ($e > 0.85$), orbital properties that seem to exclude (Gilmore and Wyse 1998) the accretion of such lightly bound systems. Another explanation is provided by the EASE scenario (Jehin et al. 1999, Jehin et al., this meeting), where it is suggested that these stars were born in (proto-) globular clusters.

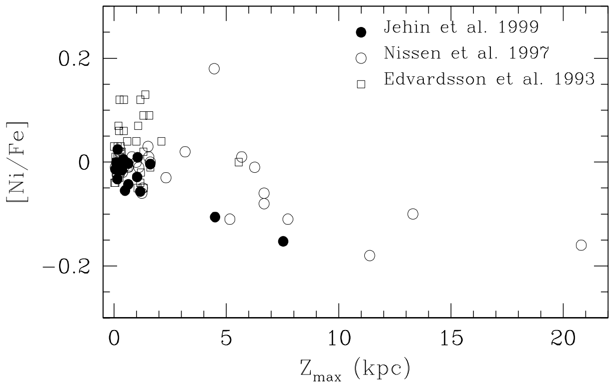

Figure 7: A clear relation between the ratio of two iron peak elements and the maximum height reached by the stars.

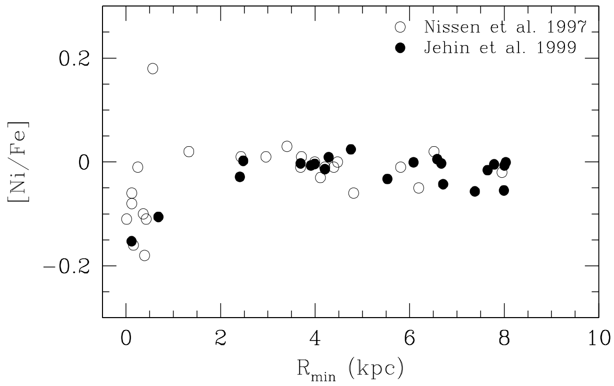

Figure 8: [Ni/Fe] versus R_{min}.

Acknowledgements

We are grateful to Dominique Naef to have made available, before publication, the CORAVEL radial velocities of our stars. This work has been supported by contracts ARC 94/99-178 “Action de Recherche Concertée de la Communauté Française de Belgique” and by the Pôle d'Attraction Interuniversitaire P4/05 (SSTC, Belgium).

References

Allen C., Santillàn A., 1991, Rev. Mex. Astron. Astrophis. 22, 255

Barbier-Brossat M., Petit M., Figon P., 1994, A&ASS 108, 603

Edvardsson B., Andersen J., Gustafsson B., Lambert D.L., Nissen P.E., Tomkin J., 1993, A&A 275, 101

ESA, 1997, “ The HIPPARCOS Catalogue ”, ESA SP-1200, ESTEC, Noordwijk

Evans D.S., 1967, “ Catalogue of Stellar Radial Velocities ”, IAU Symp. 30, 57

Gilmore G., Wyse R., 1998, AJ 116, 748

Jehin E., Magain P., Neuforge C., Noels A., Parmentier G., Thoul A.A. 1999, A&A 341, 241

Johnson D.R.H., Soderblom D.R., 1987, AJ 93, 864

Johnston K.V., Hernquist L., Bolte M., 1996, ApJ 465, 278

Mayor M., 1985, “ Stellar Radial Velocities ”, IAU Symp. 88, 35

Mihalas D., Routly P.M., 1968, “ Galactic Astronomy ”, Freeman and Co.

Nissen P.E., Schuster W.J., 1997, A&A 326, 751

Truron C., Crézé M., Egret D. et al. 1992, “ The HIPPARCOS Input Catalogue ”, ESA, Noordwijk

Wilson R.E. 1953, “ General Catalogue of Stellar Radial Velocities ”, Carnegie Inst. of Washington, Washington, D.C.